

Article

Palladium Complexes Derived from Waste as Catalysts for C-H Functionalisation and C-N Bond Formation

Khairil A. Jantan ^{1,2}, Gregor Ekart ¹, Sean McCarthy ¹, Andrew J. P. White ¹, D. Christopher Braddock ¹, Angela Serpe ³ and James D. E. T. Wilton-Ely ^{1,*}

¹ Department of Chemistry, Imperial College, Molecular Sciences Research Hub, White City Campus, London W12 0BZ, UK; khairil0323@uitm.edu.my (K.A.J.); gregor.ekart15@imperial.ac.uk (G.E.); c.braddock@imperial.ac.uk (D.C.B.)

² Faculty of Applied Sciences, Universiti Teknologi MARA (UiTM), Shah Alam 40450, Malaysia

³ Department of Civil and Environmental Engineering and Architecture (DICAAR), INSTM Unit, University of Cagliari, Via Marengo 2, 09123 Cagliari, Italy; serpe@unica.it

* Correspondence: j.wilton-ely@imperial.ac.uk

Abstract: Three-way catalysts (TWCs) are widely used in vehicles to convert the exhaust emissions from internal combustion engines into less toxic pollutants. After around 8–10 years of use, the declining catalytic activity of TWCs causes them to need replacing, leading to the generation of substantial amounts of spent TWC material containing precious metals, including palladium. It has previously been reported that $[N^nBu_4]_2[Pd_2I_6]$ is obtained in high yield and purity from model TWC material using a simple, inexpensive and mild reaction based on tetrabutylammonium iodide in the presence of iodine. In this contribution, it is shown that, through a simple ligand exchange reaction, this dimeric recovery complex can be converted into $PdI_2(dppf)$ ($dppf = 1,1'$ -bis(diphenylphosphino)ferrocene), which is a direct analogue of a commonly used catalyst, $PdCl_2(dppf)$. $[N^nBu_4]_2[Pd_2I_6]$ displayed high catalytic activity in the oxidative functionalisation of benzo[*h*]quinoline to 10-alkoxybenzo[*h*]quinoline and 8-methylquinoline to 8-(methoxymethyl)quinoline in the presence of an oxidant, $PhI(OAc)_2$. Near-quantitative conversions to the desired product were obtained using a catalyst recovered from waste under milder conditions (50 °C, 1–2 mol% Pd loading) and shorter reaction times (2 h) than those typically used in the literature. The $[N^nBu_4]_2[Pd_2I_6]$ catalyst could also be recovered and re-used multiple times after the reaction, providing additional sustainability benefits. Both $[N^nBu_4]_2[Pd_2I_6]$ and $PdI_2(dppf)$ were also found to be active in Buchwald–Hartwig amination reactions, and their performance was optimised through a Design of Experiments (DoE) study. The optimised conditions for this waste-derived palladium catalyst (1–2 mol% Pd loading, 3–6 mol% of $dppf$) in a bioderived solvent, cyclopentyl methyl ether (CPME), offer a more sustainable approach to C-N bond formation than comparable amination protocols.

Keywords: palladium; recovered metals; C-H functionalisation; C-N amination; sustainability



Citation: Jantan, K.A.; Ekart, G.; McCarthy, S.; White, A.J.P.; Braddock, D.C.; Serpe, A.; Wilton-Ely, J.D.E.T. Palladium Complexes Derived from Waste as Catalysts for C-H Functionalisation and C-N Bond Formation. *Catalysts* **2024**, *14*, 295. <https://doi.org/10.3390/catal14050295>

Academic Editor: Jacques Muzart

Received: 25 March 2024

Revised: 22 April 2024

Accepted: 25 April 2024

Published: 29 April 2024



Copyright: © 2024 by the authors. Licensee MDPI, Basel, Switzerland. This article is an open access article distributed under the terms and conditions of the Creative Commons Attribution (CC BY) license (<https://creativecommons.org/licenses/by/4.0/>).

1. Introduction

Palladium-mediated reactions are among the most frequently employed transformations in synthetic chemistry and are used widely for C-C, C-N and C-O bond formation [1–6]. However, the extremely low natural abundance of palladium in the Earth's crust, its limited distribution and geopolitical factors threaten future supply [7]. This has led to a substantial palladium deficit due to the high demand and limited supply [8]. The route of this metal from ore to its application in numerous fields features many acknowledged environmental repercussions on water and air quality, biodiversity, and population displacement [9–11]. Furthermore, the low palladium content in unrefined ore (<10 g/tonne) requires energy-intensive treatments (3880 kg CO₂e per kg of Pd [9]) in the pyrometallurgical extraction process [12], which involves smelting in blast and electric furnaces at high temperatures

require much less energy and are based on a feedstock that can contain up to 200 times more palladium than in mined ore. A recent cost analysis for catalysts based on recovered gold [23] illustrated that even unoptimized, small-scale production of the catalyst leads to a significantly lower cost than commercial catalysts derived from environmentally damaging mining.

In this contribution, we present the use of the dimer $[\text{N}^n\text{Bu}_4]_2[\text{Pd}_2\text{I}_6]$ (**1**) as an even more effective and sustainable catalyst for oxidative functionalisation reactions, such as those shown in Figure 1. Compound **1** is obtained selectively from mixed-metal model TWC material in over 70% yield using a low-energy route based on the reaction with iodine in the presence of organic iodides (such as $[\text{N}^n\text{Bu}_4]\text{I}$), as shown in Figure 2 [24]. Selective precipitation of **1** from the organic solvent (typically acetone or MIBK) allows separation from the other metals present in TWCs. The inexpensive reagents and low-energy conditions are a substantial improvement over the use of $\text{Me}_2\text{dazdt}\cdot 2\text{I}_2$; however, the process of returning the Pd content of **1** to its metallic form is still energy-intensive and thus costly. Therefore, a more effective way of valorising this recovery product is to use it directly (or with simple modification) in catalysis [16,25,26]. This is a strategy that led to the first direct application in homogeneous catalysis of gold recovery products sourced from e-waste [23]. Using simple ligand exchange reactions, $\text{PdI}_2(\text{dppf})$ (**2**), the iodide analogue of the well-known catalyst, $\text{PdCl}_2(\text{dppf})$, was synthesised from compound **1** to provide a phosphine-supported derivative. The results obtained for oxidative C-H functionalisation and Buchwald–Hartwig amination reactions using **1** and **2** are compared both in terms of catalytic activity and sustainability.

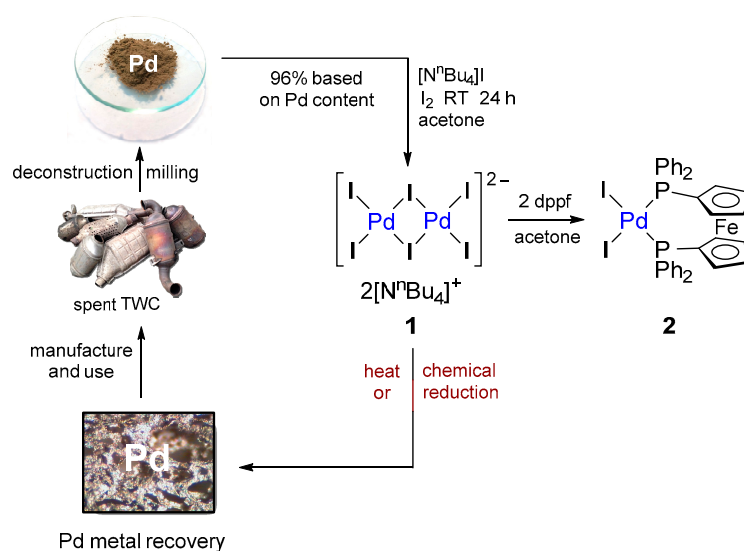


Figure 2. Palladium recovery process from TWCs to form **1** and the ligand exchange reaction used to prepare **2**.

2. Results and Discussion

2.1. Synthesis of Palladium Complexes

Complex **1** is the main product obtained from the selective Pd leaching and recovery process carried out on model samples of spent TWC using tetrabutylammonium iodide in the presence of iodine in an acetone solution [24] (Figure 2). The iodine/iodide system offers a ‘greener’ approach to Pd recovery compared to traditional pyrometallurgical or hydrometallurgical processes due to its versatility, mild conditions, minimal environmental impact, use of inexpensive reagents and easily recyclable solvents. These attributes also allow it to be employed in low-income regions where there is currently no local recycling infrastructure for TWCs. Since the use of $[\text{N}^n\text{Bu}_4]\text{I}/\text{I}_2$ to recover Pd from model TWC material is already well established [24], compound **1** was obtained directly by leaching palladium metal on a small scale using the same reagents. The black crystalline product

(86% yield) was usually obtained by Et₂O diffusion into the acetone leachate over a period of 3 days. A more rapid crystallisation process was also used to obtain a less crystalline but analytically identical product through the addition of ethanol and concentration of the solvent volume until precipitation had been achieved. Compound **1** obtained from both approaches leads to characteristic features in the UV-vis spectrum at 2960–2869 cm⁻¹, 1457 and 1379 cm⁻¹, with the latter two absorptions attributed to the tetrabutylammonium units. The presence of the dimeric palladium complex [Pd₂I₆]²⁻ was indicated by an absorption at 340 nm. The overall formulation was confirmed by an abundant molecular ion in the electrospray (negative ion) mass spectrum at *m/z* 487 (ESI, Section S1.2) and good agreement of the elemental analysis with calculated values.

Palladium phosphine complexes are the most widely used ligand-supported (pre)catalysts [4–6,16,27], with PdCl₂(dppf) being used in many settings, including for Buchwald–Hartwig amination reactions [28]. Thus, the recovery complex [NⁿBu₄]₂[Pd₂I₆] (**1**) was treated with dppf in acetone to produce the iodide analogue, PdI₂(dppf) (**2**), in 97% yield. A singlet was observed in the ³¹P{¹H} NMR spectrum at 24.3 ppm, while the presence of the dppf ligands was clearly observed in the ¹H NMR spectrum through ferrocenyl resonances at 4.14 and 4.35 ppm. In addition, typical aromatic features were observed in the solid-state FTIR spectrum (1092 and 1480 cm⁻¹) and the overall composition was confirmed by mass spectrometry (ESI, Section S1.3) and elemental analysis. Crystals suitable for single-crystal X-ray diffraction measurements were obtained through the slow diffusion of ethanol into a chloroform solution of PdI₂(dppf) (Figure 3). This revealed a distorted square planar arrangement at the Pd(II) centre due to the steric requirement of the bulky dppf ligand. The bond lengths and angles are similar to those reported for the same complex in a lower-quality structure in 2001 [29]. Further discussion and crystal data are provided in the ESI (Section S2).

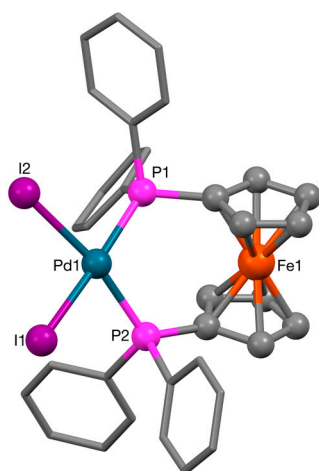


Figure 3. Molecular structure of **2**. Selected bond lengths (Å) and angles (°): Pd(1)–I(1) 2.6495(5), Pd(1)–I(2) 2.6454(6), Pd(1)–P(1) 2.3281(13), Pd(1)–P(2) 2.3245(15), P(2)–Pd(1)–I(1) 83.83(3), P(1)–Pd(1)–I(2) 88.60(4), P(1)–Pd(1)–P(2) 99.77(5).

2.2. Oxidative C–H Functionalisation

Palladium(II) compounds are known to catalyse a variety of oxidative C–H functionalisation processes, particularly the conversion of benzo[*h*]quinoline to 10-alkoxybenzo[*h*]quinoline [2,3,21,22]. The catalytic potential of recovery product **1** and its derivative **2** was assessed for this class of transformation using the conversion of benzo[*h*]quinoline to 10-methoxybenzo[*h*]quinoline as a benchmark reaction (Figure 1). The term ‘conversion’ will be used here rather than yield, as the amount of desired product formed was determined using ¹H NMR spectroscopy, rather than as an isolated yield of each product. NMR spectroscopy has been shown [21] to allow sufficient accuracy (2–5% error) to determine the impact of changes in the reaction conditions on the formation of the product. Isolated

yields have been reported previously and show only a small decrease compared to the conversion determined spectroscopically [21]. The conditions reported in the literature for this transformation were used (1.1 mol% catalyst loading, 2 equivalents $\text{PhI}(\text{OAc})_2$, 100 °C, 22 h). Under these conditions, complexes **1** and **2** provided near-quantitative conversions to the desired product, as determined by ^1H NMR spectroscopy (97 and 96%, respectively), of 10-methoxybenzo[*h*]quinoline, competing favourably with the 96% yield reported in the literature (and confirmed here) using $\text{Pd}(\text{OAc})_2$, sourced from conventional mining (ESI, Section S4). These results also matched those we previously reported for $[\text{Pd}(\text{Me}_2\text{dazdt})_2][\text{I}_3]_2$ [21]. The proposed mechanism [22,30] for these reactions involves a Pd(II)-Pd(IV) manifold, though Pd(III) intermediates have also been postulated [31].

Heating methanol at 100 °C in a sealed vessel for 22 h leads to both safety and sustainability concerns and so attempts were made to perform the reaction under milder conditions. Following the initial screening reactions, the product conversion over time was investigated for the methoxylation of benzo[*h*]quinoline at different temperatures, first using the literature catalyst $\text{Pd}(\text{OAc})_2$ at a loading of 1.1 mol% (Figure 4). At high temperatures (100 °C), no induction period was observed, with the fastest rate of reaction occurring at the start of the reaction. However, heating flammable solvents above their boiling point in a confined space generates potential danger related to pressure build-up. At the lower temperature of 50 °C, the $\text{Pd}(\text{OAc})_2$ reaction proceeds more slowly but then achieves 86% conversion to 10-methoxybenzo[*h*]quinoline after 5 h before reaching 95% after 22 h, a conversion reached in only 2 h at 100 °C (ESI, Table S4-1). Perhaps due to a tendency to use established protocols involving longer reaction times, it appears that previous investigations did not reveal that high yields were already formed after much shorter reaction times.

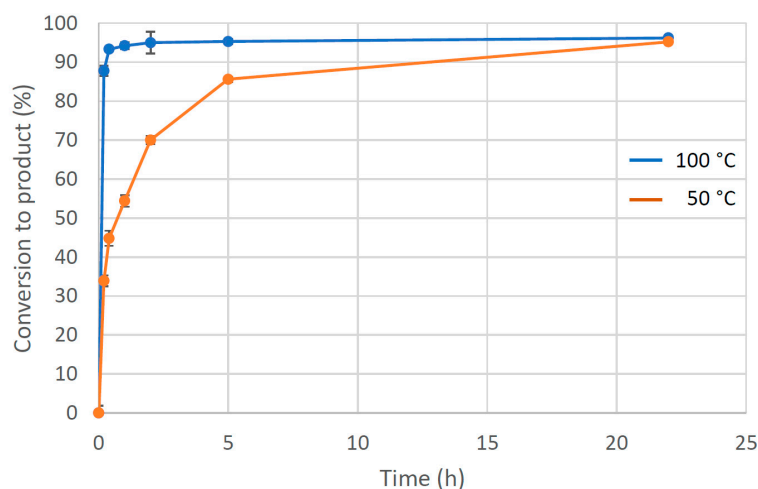


Figure 4. Formation of 10-methoxybenzo[*h*]quinoline from benzo[*h*]quinoline over time using 1.1 mol% $\text{Pd}(\text{OAc})_2$ in the presence of $\text{PhI}(\text{OAc})_2$ in MeOH at 100 °C (blue line) and 50 °C (orange line). Conversion was determined from an average of three independent experiments by comparing the integration of H-2 and H-10 resonances in benzo[*h*]quinoline with the diagnostic methoxy resonance in the 10-methoxybenzo[*h*]quinoline product.

The appearance of a black residue at the bottom of the vials used in the reaction at 100 °C after 22 h was noted, and this material was analysed using transmission electron microscopy (TEM). This ‘palladium black’ was revealed to also contain palladium nanoparticles (Figure 5A) with an average diameter of 2.6 nm and a relatively broad size distribution of ± 1.1 nm. Though palladium nanoparticles (PdNPs) are well known to catalyse many Pd(0)-mediated reactions, such as Suzuki–Miyaura couplings [32], they have also been observed in C-H functionalisation reactions [33,34]. The formation of the PdNPs was investigated in separate control experiments (ESI, Section S3.2.1), in which $\text{Pd}(\text{OAc})_2$ was heated for 22 h at 100 °C in a methanol solution with or without $\text{PhI}(\text{OAc})_2$ to yield pal-

ladium nanoparticles with an average diameter of 1.2 nm (± 0.3 nm) and 1.5 nm (± 0.5 nm), respectively (Figure 5B,C). The presence of the sacrificial oxidant does not appear to prevent the reduction of Pd(OAc)₂. These results suggest that the Pd(OAc)₂ catalyst undergoes (at least partial) in situ reduction in the alcohol solution to produce PdNPs under the reaction conditions for C-H functionalisation.

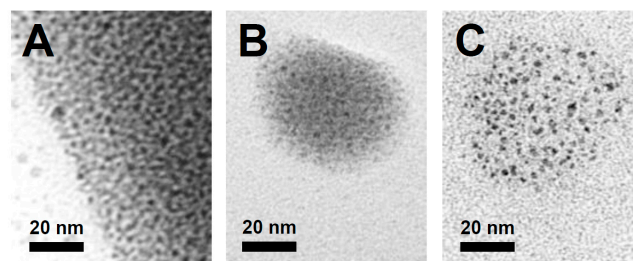


Figure 5. TEM images of Pd nanoparticles obtained (A) after methoxylation of benzo[*h*]quinoline using Pd(OAc)₂ as a catalyst, (B) after Pd(OAc)₂ was heated with the sacrificial oxidant PhI(OAc)₂ in methanol and (C) after heating Pd(OAc)₂ in methanol. All reactions were conducted at 100 °C for 22 h.

Further investigation was carried out to investigate whether the formation of palladium nanoparticles aided or hindered the methoxylation of benzo[*h*]quinoline. Palladium acetate was heated in methanol in air for 2 h at 100 °C followed by the addition of benzo[*h*]quinoline and PhI(OAc)₂ to the solution. The reaction mixture was stirred and heated at 100 °C for another 22 h. A 67% conversion to 10-methoxybenzo[*h*]quinoline was obtained after 22 h of reaction, which is substantially lower than the 95% obtained without the initial heating step in methanol. One suggestion is that a fraction of Pd(OAc)₂ survives the reduction to Pd nanoparticles and is then able to catalyse the C-H functionalisation reaction. Alternatively, as proposed by Fairlamb and co-workers [33,34], the PdNPs formed could be acting as a ‘reservoir’ of active Pd that performs the transformation but the larger PdNPs formed are inactive. The palladium black that can be observed by the naked eye consists of much larger, micrometre-sized particles, which are themselves unlikely to be catalytically active. Taken together, these results suggest that the use of Pd(OAc)₂ at high temperatures in an alcohol solvent, as reported in the literature [22], actually contributes to the deactivation of the catalyst and that the good conversions obtained after 22 h were actually due to the residual catalytic species that managed to operate under the conditions employed.

Following this investigation of the literature catalyst, Pd(OAc)₂, the catalytic activity of [NⁿBu₄]₂[Pd₂I₆] (**1**) was explored in the functionalisation of benzo[*h*]quinoline using the conditions that had provided the highest conversions (c.f. Figure 4) over shorter reaction times (1–2 mol% [Pd] loading, 100 °C, 2 h). Near-quantitative conversions to the desired product were recorded for the selective alkoxybenzo[*h*]quinoline for two alcohols, ROH (R = Me, CH₂CF₃), using 1 mol% Pd loading. However, a two-fold increase in catalyst loading was required to provide better conversion to 10-ethoxybenzo[*h*]quinoline (81%) and 10-isopropoxybenzo[*h*]quinoline (75%) (Figure 6 and ESI, Table S4-2). The lower activity with ethanol and isopropanol could be due to the differing speciation of the active catalyst species in solvents of different polarity.

Similarly to the reactions catalysed by Pd(OAc)₂, a black residue was observed at the bottom of the reaction vials after 2 h of the reaction using [NⁿBu₄]₂[Pd₂I₆] (**1**) at 100 °C for all substrates except for the trifluoroethanol reaction mixture. The black precipitate was centrifuged, washed with methanol and dried under a vacuum. TEM images (Figure 7) revealed the formation of small palladium nanoparticles (PdNPs). Average diameters of 2.0 nm (methanol), 1.8 nm (ethanol) and 2.3 nm (mixture of isopropanol/acetic acid) were recorded, confirming that the formation of PdNPs was not exclusive to the use of Pd(OAc)₂. The lack of formation of nanoparticles in the trifluoroethanol reaction mixture could be

due to the electron-withdrawing CF_3 unit stabilising the palladium(II) complex effectively, hindering the formation of PdNPs at high temperatures.

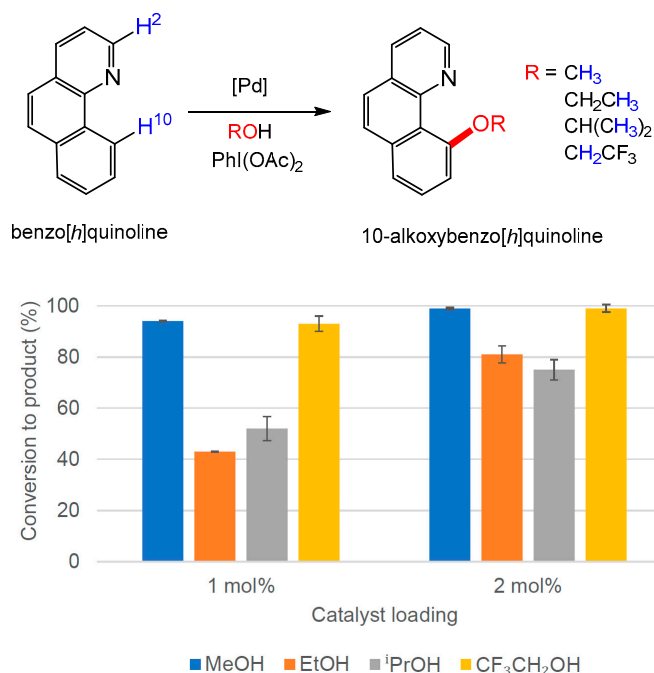


Figure 6. Results for the formation of alkoxybenzo[*h*]quinoline using **1** as a catalyst in the alcohols shown at 100 °C. The conversion to 10-alkoxybenzo[*h*]quinoline was determined by ¹H NMR spectroscopy using the average of three independent experiments by comparing the integration of H-2 and H-10 resonances in benzo[*h*]quinoline with the diagnostic resonances of methoxy, ethoxy, isopropoxy and trifluoroethoxy groups in the products. 10-isopropoxybenzo[*h*]quinoline is formed from a mixture of isopropanol and acetic acid, according to the original literature protocol [22].

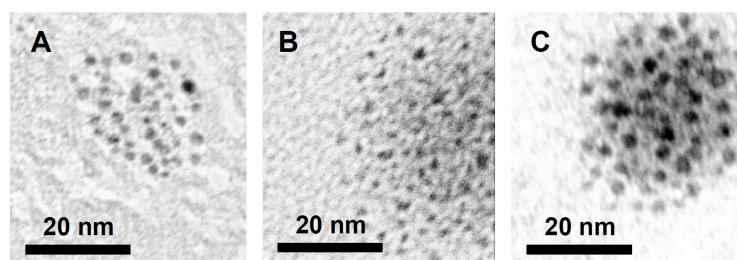


Figure 7. TEM images of Pd nanoparticles formed after heating benzo[*h*]quinoline and $\text{PhI}(\text{OAc})_2$ with **1** at 100 °C for 2 h in the presence of (A) MeOH, (B) EtOH, and (C) ⁱPrOH (and acetic acid).

The same transformations were repeated with $[\text{N}^n\text{Bu}_4]_2[\text{Pd}_2\text{I}_6]$ (**1**) as the catalyst at 50 °C while modifying the reaction conditions (loading and reaction times) to attain satisfactory conversions within an acceptable reaction time (Figure 8 and ESI Table S4-3). Significantly, in all cases at this lower temperature, there was no visual evidence for the formation of PdNPs. At 1 mol% [Pd] catalyst loading, low to moderate conversions (as determined by ¹H NMR spectroscopy) were observed (Figure 8A), which improved over longer reaction times for reactions with MeOH and $\text{CF}_3\text{CH}_2\text{OH}$. Doubling the catalyst loading to 2 mol% [Pd] led to essentially quantitative conversions to the desired product in 2 h for all products, except for 10-isopropoxybenzo[*h*]quinoline, which showed a steady increase in the conversion to 82% after 24 h (Figure 8B). A 3 mol% loading of **1** and a reaction time of 4 h were found to be necessary to achieve a high conversion (92%) to the isopropoxy-functionalised product (ESI Table S4-3). The standard operating conditions were thus defined as being 2 mol% [Pd] catalyst loading at 50 °C for 2 h. An isolated yield

of 97% of 10-methoxybenzo[*h*]quinoline was obtained using these conditions, reflecting the ease of isolation of these products through flash column chromatography.

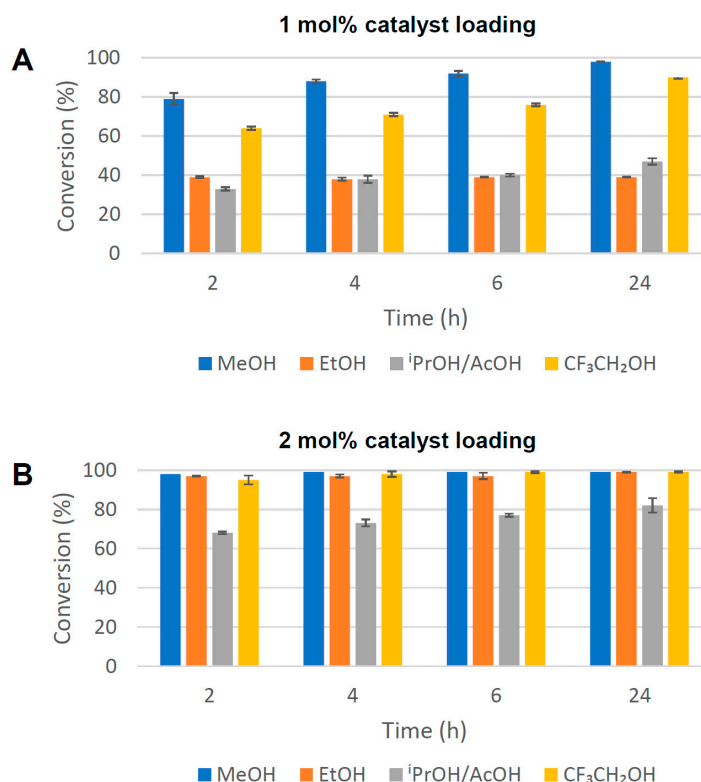
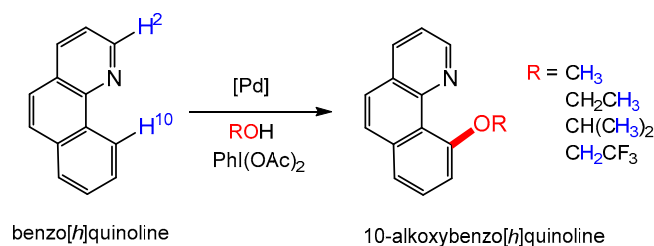


Figure 8. Alkoxy functionalisation of benzo[*h*]quinoline in different alcohol solvents at 50 °C employing **1** as a catalyst at (A) 1 mol% and (B) 2 mol% [Pd] loading. The conversion to 10-alkoxybenzo[*h*]quinoline was determined by ¹H NMR spectroscopy using the average of three independent experiments by comparing the integration of H-2 and H-10 resonances in benzo[*h*]quinoline with the diagnostic resonances of methoxy, ethoxy, isopropoxy and trifluoroethoxy groups in the products.

The same conditions were then employed to investigate the use of PdI₂(dppf) (**2**) as a catalyst for the same reaction. Using 1 mol% loading (Figure 9A), 98% conversion to 10-methoxybenzo[*h*]quinoline was obtained after only 2 h. Increasing the catalyst loading to 2 mol% (Figure 9B) improved the conversions of the more challenging reactions to produce 10-trifluoroxybenzo[*h*]quinoline (94%) and 10-isopropoxybenzo[*h*]quinoline (95%) after 4 h and 24 h, respectively (see also ESI Table S4-4).

Encouraged by the successful result for the alkoxylation of benzo[*h*]quinoline, the synthesis of 8-(methoxymethyl)quinoline from 8-methylquinoline was briefly investigated. The data obtained suggest that compound **1** appears to deliver superior catalytic performance compared to the other catalysts under investigation (ESI, Table S4-6). An isolated yield of 94% of 8-(methoxymethyl)quinoline was obtained using 1 mol% of **1** in methanol at 50 °C for 2 h following a flash column (ESI, Section S3.2.2).

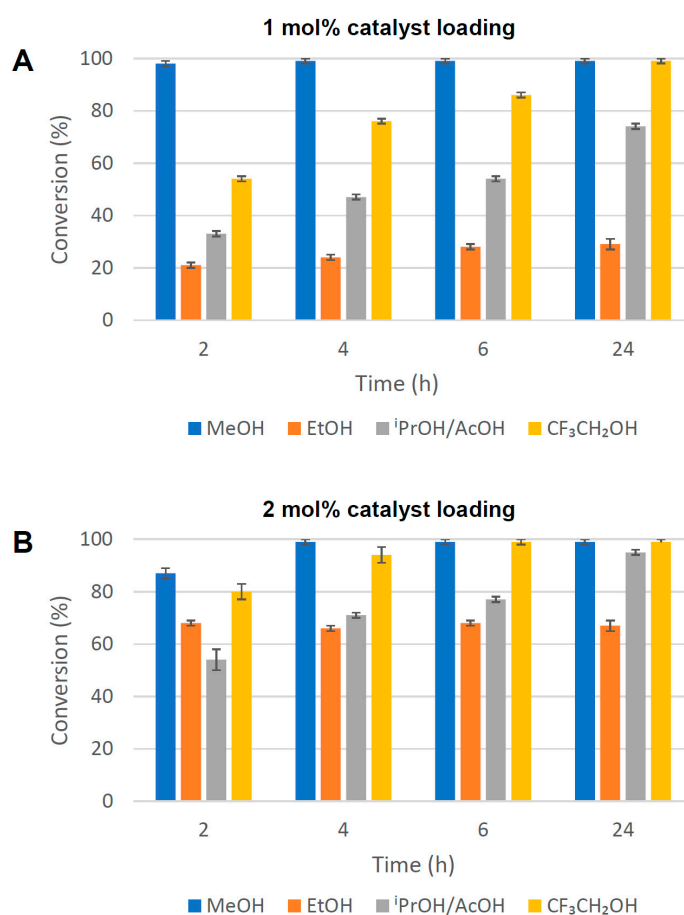
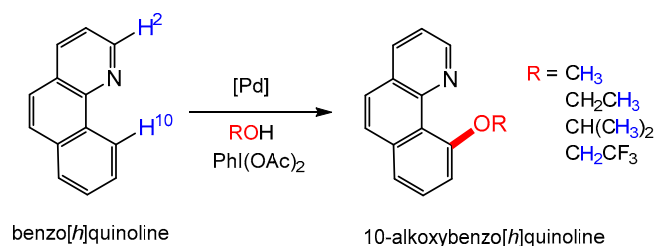
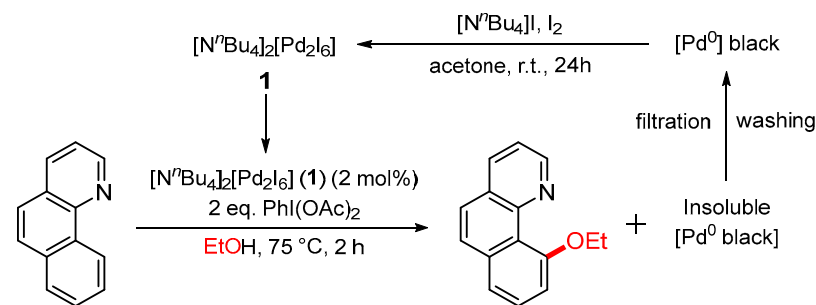


Figure 9. Alkoxy functionalisation of benzo[*h*]quinoline in different alcohol solvents at 50 °C employing PdI₂(dppf) (**2**) as a catalyst at (A) 1 mol% and (B) 2 mol% [Pd] loading. The conversion to 10-alkoxybenzo[*h*]quinoline was determined by ¹H NMR spectroscopy using the average of three independent experiments by comparing the integration of H-2 and H-10 resonances in benzo[*h*]quinoline with the diagnostic resonances of methoxy, ethoxy, isopropoxy and trifluoroethoxy groups in the products.

While the use of a recovery product obtained under mild conditions from waste as the catalyst enhances the ‘green’ credentials of the approach, recycling of the catalyst would further enhance the sustainability of the process. This was investigated briefly in the reaction to form 10-ethoxybenzo[*h*]quinoline, shown in Table 1. Conditions were optimised to produce 10-ethoxybenzo[*h*]quinoline over a shorter reaction time (2 h). This required an increase in the reaction temperature to 75 °C and the use of 2 mol% catalyst loading. A near-quantitative conversion to the desired product was obtained in the first run, with a palladium black precipitate forming within the first 30 min of the reaction. This precipitate was isolated, washed and converted back to [NⁿBu₄]₂[Pd₂I₆] (**1**) in 75% yield using the same procedure for its synthesis from Pd powder using [NⁿBu₄]I/I₂. The recovered compound **1** was used for the second run, which led to the same quantitative conversion to the 10-

ethoxybenzo[*h*]quinoline product. Following the reaction, after treatment with $[N^tBu_4]I/I_2$, compound **1** was recovered for a second time with 72% yield. This approach is being investigated further to assess the breadth of its application in different catalytic reactions.

Table 1. Use and re-use of $[N^tBu_4]_2[Pd_2I_6]$ (**1**) in the synthesis of 10-ethoxybenzo[*h*]quinoline. The second run was scaled down so that a loading of 2 mol% of recovered **1** was maintained. Conversion to the product was determined by 1H NMR spectroscopy by comparing the integration of H-2 and H-10 resonances in benzo[*h*]quinoline with the diagnostic ethoxy resonances in the product and also with an internal standard, 1,3,5-trimethoxybenzene. The recovery (isolated) yield was calculated with respect to the amount of **1** in the reaction mixture.



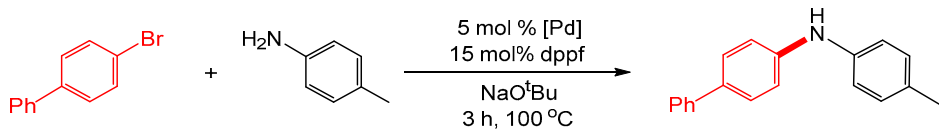
Run	Conversion to organic product (%)	Recovery yield of 1 (%)
1	97	75
2	98	72

2.3. Amination Reactions

The palladium-catalysed Buchwald–Hartwig amination reaction is an essential tool in organic synthesis and in the pharmaceutical industry in particular [4,35–39]. Pioneering work by Hartwig demonstrated that a range of amination reactions could be catalysed by $PdCl_2(dppf)$ in the presence of additional dppf in an inert environment [28]. The similarities between $PdCl_2(dppf)$ and the $PdI_2(dppf)$ (**2**) generated from the $[N^tBu_4]_2[Pd_2I_6]$ (**1**) recovery product provided encouragement to explore the possibility of substituting current catalysts with more sustainable alternatives derived from waste. In addition, our aim was also to enhance the sustainability still further by exploring ‘greener’ solvents and more straightforward conditions that do not require the exclusion of oxygen and moisture. In order to explore these aspects, complexes **1** and **2** were applied to the benchmark cross-coupling reaction of *p*-bromobiphenyl and *p*-toluidine in a range of solvent systems in air (Table 2), following literature protocols (5 mol% Pd loading, 15 mol% dppf ancillary ligand and sodium *tert*-butoxide as a base for 3 h at 100 °C). The methyl resonances in *p*-toluidine (2.24 ppm) and the product (2.33 pm) were employed as characteristic 1H NMR spectroscopic features to monitor the reaction through integration of the respective signals.

The experimental protocol in the original report [28] described heating at 100 °C in tetrahydrofuran for 3 h using 5 mol% Pd loading and 15 mol% dppf as an ancillary ligand. The runs using these conditions were performed in a high-pressure vial due to the significantly lower boiling point of the THF solvent (66 °C). Compounds **1** and **2** showed lower catalytic activity compared to the $PdCl_2(dppf)$ in this initial set of experiments (Table 2). However, heating THF above its boiling point poses a safety risk due to increased pressure. Thus, solvents with higher boiling points were explored, such as toluene (b.p. 111 °C) and cyclopentyl methyl ether (CPME, b.p. 106 °C). Conducting the reaction in these solvents led to improved conversions (Table 2) for reactions catalysed by **1** and **2** as well as high conversions for the commercial palladium catalyst, $PdCl_2(dppf)$. This was the first indication that $PdI_2(dppf)$ (**2**), obtained from a palladium recovery pathway, was able to deliver comparable catalytic performance to the literature catalyst.

Table 2. Solvent screening for the benchmark reaction of *p*-bromobiphenyl and *p*-toluidine in the presence of 5 mol% Pd loading and 15 mol% dppf at 100 °C for 3 h using different catalysts. The conversion to the desired product was determined by ¹H NMR spectroscopy by comparing the integration of diagnostic methyl resonances in *p*-toluidine and the product, taking into account the excess of *p*-toluidine used. Values are the average of three independent experiments. CPME = cyclopentyl methyl ether.



Solvent	Conversion (%) with PdCl ₂ (dppf)	Conversion (%) with [N ⁿ Bu ₄] ₂ [Pd ₂ I ₆] (1)	Conversion (%) with PdI ₂ (dppf) (2)
THF	90 ± 1	55 ± 1	81 ± 1
CPME	98 ± 1	92 ± 2	90 ± 1
Toluene	98 ± 1	80 ± 1	96 ± 2

In addition to its favourable properties, including low toxicity, high boiling point, low melting point, hydrophobicity and chemical stability, cyclopentyl methyl ether (CPME) can also be bio-derived from furfural [40]. It is known to broadly mimic the chemical properties of both THF and toluene, but with a lower environmental and health score [41]. On the basis of this improved sustainability and the high conversions it delivered for **1** and **2**, this solvent was chosen to be taken forward as a solvent for the remainder of this work. It was also determined that carrying out the reaction in air did not affect the conversion to the desired product when compared to an anhydrous CPME solution.

Ancillary ligands, such as electron-rich and bulky dppf ligands, are often required in amination reactions to increase the rate of the reaction, prevent the formation of palladium halide dimers after oxidative addition [27,28], and suppress β-hydride elimination by preventing an open coordination site [36]. Without additional equivalents of the dppf ligand, no product formation was observed under the conditions described above. Since PdI₂(dppf) (**2**) is readily obtained from [NⁿBu₄]₂[Pd₂I₆] (**1**) and dppf, the in situ generation of **2** was also investigated, as discussed below.

The catalytic performance of **1** and **2** towards the aryl iodide analogue, *p*-iodobiphenyl, was explored in CPME. In contrast to the aryl bromides, the catalytic activities of all catalysts appeared to be adversely affected by the switch to aryl iodide substrates, providing a lower conversion to the desired product (Table 3). This result agreed with the previously reported literature [35,37] suggesting that aryl iodides are less effective substrates than their aryl bromide counterparts in amination reactions. This has been suggested to be connected to the poisoning of the catalyst through the accumulation of iodide salts in the reaction medium [38].

Table 3. Reaction of *p*-iodobiphenyl and *p*-toluidine in the presence of 15 mol% dppf at 100 °C for 3 h using different catalysts at 2 and 5 mol% palladium loadings. The conversion to the desired product was determined by ¹H NMR spectroscopy by comparing the integration of diagnostic methyl resonances in *p*-toluidine and the product, taking into account the excess of *p*-toluidine used. Values are the average of three independent experiments.

Pd loading (mol%)	Conversion (%) with PdCl ₂ (dppf)	Conversion (%) with [N ⁿ Bu ₄] ₂ [Pd ₂ I ₆] (1)	Conversion (%) with PdI ₂ (dppf) (2)
5	71 ± 3	59 ± 1	65 ± 3
2	80 ± 1	72 ± 1	57 ± 2

While encouraging, these results suggest that a lower catalyst loading than 5 mol% could actually be beneficial and that the reaction conditions still had room for improvement. Accordingly, we sought to optimise the conversion to the desired product for the benchmark reaction with catalyst **2** through an investigation of key variables using a 'Design

of Experiments' (DoE) strategy, guided by JMP Statistical Discovery software. Definitive screening designs considered three factors at three levels, the minimum, centre and maximum, with a total of 20 test runs (ESI, Table S3-1). The results obtained (ESI, Table S5-1) were used to build a model to predict the outcome of the reaction and possible variable combinations of catalyst loading, dppf loading and reaction time. The results of this study (ESI, Table S3-2) indicate that the individual effect of time is the most significant parameter, followed by two-factor interactions of catalyst loading with time and dppf loading, in that order. Only slightly below this were the effects of catalyst loading and dppf amount. Figure 10A shows the relationships between the experimental and predicted conversions to the desired product. This graph helps to illustrate the error and the performance of the model. The data points should be split evenly by the 45-degree line to test the model's fit. The quality fit of the model equation was expressed by the coefficient regression (R^2) as 0.97, which is close to unity, signifying a good fit of experimental data to the model, providing confidence that it can predict the product yield.

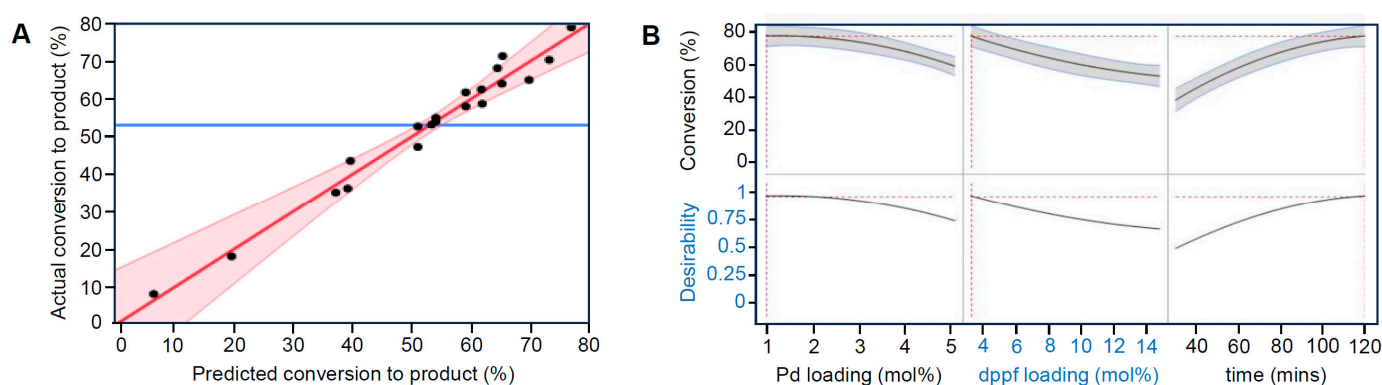


Figure 10. (A) Predicted and actual conversion to the desired product for the DoE model and (B) predicted optimal conditions (1 mol% Pd, 3 mol% dppf, 120 min) for the benchmark reaction between *p*-bromobiphenyl and *p*-toluidine at 100 °C in CPME solution, as extracted from definitive screening design variable profiles.

The DoE analysis shown in Figure 10B indicates that the optimal predicted reaction yield for the reaction in CPME solution at 100 °C will be provided by 1 mol% PdI₂(dppf) (2) loading and 3 mol% dppf in 120 min. This confirmed that, while a 1:3 ratio of [Pd] to [dppf] was optimal, the palladium loading could be lowered significantly from the 5 mol% PdCl₂(dppf) typically used in the literature.

Kinetic experiments were conducted to investigate the conversion to the desired product over time and to better understand the behaviour of 2 as a catalyst in the model reaction (Figure 11 and ESI Table S5-2). This graph shows that no significant induction period was observed, with the fastest rate of reaction occurring at the start of the experiment. Extending the reaction time from 120 to 180 min led to only a slight increase in conversion to the product.

After establishing a set of catalytic conditions optimised for the reaction between *p*-toluidine and *p*-bromobiphenyl (1 mol% [Pd] loading, 3 mol% dppf at 100 °C for 3 h in CPME), the substrate scope was briefly explored with various aryl bromides (Table 4), keeping the toluidine constant. Both pre-formed PdI₂(dppf) (2) and 2 formed in situ from [NⁿBu₄]₂[Pd₂I₆] (1) and dppf were explored. For the in situ reactions, all reagents were combined and heating commenced without any catalyst pre-formation period. Overall, it was clear that the optimised catalytic conditions for the reaction between *p*-bromobiphenyl and *p*-toluidine (1 mol% [Pd]) proved insufficient to provide good conversions for all the substrates investigated in the subsequent substrate scope study. However, moving to 2 mol% [Pd] led to improved conversions to the desired product across the substrates explored both for pre-formed PdI₂(dppf) (2) and when 2 was generated in situ.

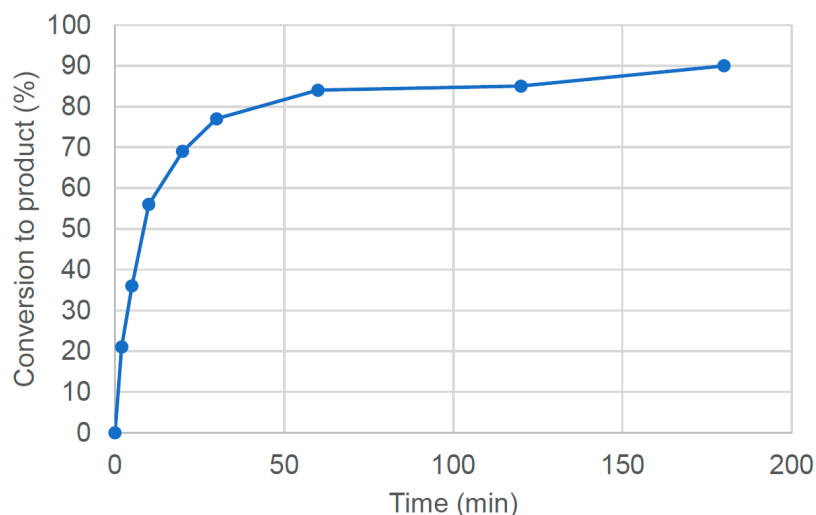
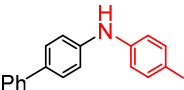
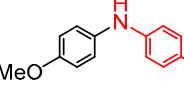
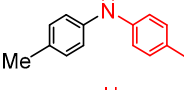
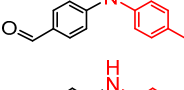
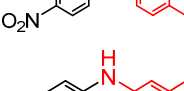
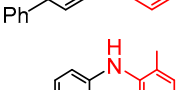
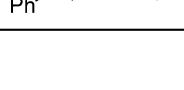


Figure 11. Reaction profile for the reaction between *p*-bromobiphenyl and *p*-toluidine at 100 °C in CPME in the presence of 1 mol% PdI₂(dppf) (**2**) and 3 mol% dppf. The conversion to the desired amination product was determined by ¹H NMR spectroscopy by comparing the integration of diagnostic methyl resonances in the product with an internal standard, 1,3,5-trimethoxybenzene. Values are the average of three independent experiments.

Table 4. Conversion to the products shown for various aromatic amines and aryl bromides after the reaction at 100 °C in CPME for 3 h in the presence of different [Pd] loadings of [NⁿBu₄]₂[Pd₂I₆] (**1**) or PdI₂(dppf) (**2**) and the stated amount of dppf. When using **1**, sufficient dppf was used to generate **2** in situ with the stated [Pd]:[dppf] ratio. The conversions to the desired products are an average of three independent experiments and were determined by ¹H NMR spectroscopy using relative integrations and 1,3,5-trimethoxybenzene as an internal standard (see ESI Section S3.3.7).

Conversion to the Product Shown (%)					
	Catalyst 2 1 mol% [Pd] 3 mol% [dppf]	Catalyst 1 1 mol% [Pd] 3 mol% [dppf]	Catalyst 2 2 mol% [Pd] 6 mol% [dppf]	Catalyst 1 2 mol% [Pd] 6 mol% [dppf]	Catalyst 2 2 mol% [Pd] 15 mol% [dppf]
	85 ± 2	83 ± 1	99 ± 1	99 ± 1	99 ± 1
	0	0	45 ± 2	60 ± 1	98 ± 2
	19 ± 3	26 ± 2	80 ± 1	96 ± 2	85 ± 2
	17 ± 2	35 ± 3	17 ± 2	21 ± 4	45 ± 1
	62 ± 4	59 ± 1	81 ± 2	97 ± 1	87 ± 1
	15 ± 1	-	99 ± 1	86 ± 3	91 ± 1
	9 ± 2	-	82 ± 2	82 ± 2	95 ± 2

This higher loading helped to improve the conversion for more sterically hindered substrates, such as *ortho*-toluidine. However, *para*-bromobenzaldehyde proved a challenging substrate across all conditions employed, though a slightly improved conversion was obtained upon increasing the [Pd]:[dppf] ratio to 1:7.5 from 1:3. This change in conditions also benefitted the reaction with *para*-bromoanisole, resulting in a conversion to the desired product of 98%.

3. Materials and Methods

Synthesis and catalytic testing details are provided in the Supplementary Materials along with spectroscopic, crystallographic and analytical characterisation data. Tables are also included for the catalytic data presented in the plots in the main text.

4. Conclusions

Palladium catalysis continues to play a central role in metal-mediated transformations in synthetic chemistry, yet its widespread use is currently dependent on palladium sourced from mining, with all its attendant environmental and geopolitical issues. The low abundance of the metal and its limited geographical distribution encourages the greater recovery and re-use of the palladium-containing waste in our society, principally in the form of three-way catalysts (TWCs). This contribution draws on an effective and mild route to recover palladium in the form of the dimer $[N^nBu_4]_2[Pd_2I_6]$ (**1**) using inexpensive compounds, $[N^mBu_4]I$, I_2 and acetone.

In this work, compound **1** has been shown to be an effective oxidative C-H functionalisation catalyst, providing near-quantitative conversions to the desired product in the alkoxylation of benzo[*h*]quinoline and 8-methylquinoline, in most cases under significantly milder conditions, lower loading and shorter reaction times (50 °C, 1–2 mol% Pd loading, 2 h) than those reported in the literature [22]. The sustainability of the reaction was further enhanced by the demonstration that the palladium black formed after the reaction could be converted to $[N^mBu_4]_2[Pd_2I_6]$ (**1**) using $[N^mBu_4]I/I_2$ and re-used as a catalyst multiple times. The higher temperature typically used in previous reports (100 °C) was found to lead to the formation of Pd nanoparticles with both $Pd(OAc)_2$ (the literature catalyst) and **1**, which had a negative impact on the catalyst performance. The addition of dppf to compound **1** led to the formation of $PdI_2(dppf)$ (**2**) in high yield, allowing it to be used as a more sustainable alternative catalyst to the $PdCl_2(dppf)$ often used in Buchwald–Hartwig amination reactions. Optimisation of the conditions allowed a lower catalyst loading (1–2 mol% depending on the substrate) to be employed in a greener, bioderived solvent, cyclopentyl methyl ether (CPME). Catalyst **2** could also be generated in situ through the addition of dppf to $[N^mBu_4]_2[Pd_2I_6]$ (**1**), leading to similar conversions to the desired product.

In addition to sustainability improvements (milder conditions, greener solvents), this contribution illustrates the potential to replace palladium catalysts derived from mining with alternatives that can be obtained from waste under mild conditions. The use of **1** and **2** for two important palladium-catalysed transformations (C-H functionalisation and amination) bodes well for the same approach to be applied to other key Pd-mediated reactions, thus improving the sustainability of palladium catalysis.

Supplementary Materials: The following supporting information can be downloaded at: <https://www.mdpi.com/article/10.3390/catal14050295/s1>. Figure S1-1. Solid-state infrared spectrum of $[N^mBu_4]_2[Pd_2I_6]$ (**1**); Figure S1-2. Mass spectrum of $[N^mBu_4]_2[Pd_2I_6]$ (**1**); Figure S1-3. UV-Vis spectrum of $[N^mBu_4]_2[Pd_2I_6]$ (**1**) in MeCN; Figure S1-4. Solid-state infrared spectrum for $PdI_2(dppf)$ (**2**); Figure S1-5. 1H NMR spectrum of $PdI_2(dppf)$ (**2**) in $CDCl_3$; Figure S1-6. $^{31}P\{^1H\}$ NMR spectrum of $PdI_2(dppf)$ (**2**) in $CDCl_3$; Figure S1-7. Mass spectrum of $PdI_2(dppf)$ (**2**); Figure S2-1. The crystal structure of **2** (50% probability ellipsoids); Figure S3-1. Reaction setup for catalytic reactions; Figure S3-2. 1H NMR spectrum in $CDCl_3$ of the reaction mixture after the formation of 10-methoxybenzo[*h*]quinoline from benzo[*h*]quinoline showing the calculation of conversion using integration of the proton environments in the starting material and the product; Figure S3-3. 1H NMR spectrum in $CDCl_3$ of isolated 10-methoxybenzo[*h*]quinoline; Figure S3-4. 1H NMR spec-

trum in CDCl_3 of isolated 8-(methoxymethyl)quinoline; Figure S3-5. HPLC calibration curve of product against 1,3,5-trimethoxybenzene internal standard; Figure S3-6. HPLC calibration curve of *p*-bromobiphenyl against 1,3,5-trimethoxybenzene internal standard; Table S3-1. Definitive screening design parameters used in the Design of Experiments (DoE) model for the reaction of *p*-bromobiphenyl and *p*-toluidine at 100 °C in CPME solution; Table S3-2. Terms included in the definitive screening design model and their corresponding LogWorth values with larger values indicate a larger influence on the model. Terms with a LogWorth < 2 are not statistically significant and are not included; Table S4-1. Reaction profile for the conversion of benzo[*h*]quinoline to 10-methoxybenzo[*h*]quinoline with $\text{Pd}(\text{OAc})_2$ (1.1 mol%) in the presence of 2 equivalents of $\text{PhI}(\text{OAc})_2$ in MeOH at 50 °C and 100 °C; Table S4-2. Transformation of benzo[*h*]quinoline to 10-alkoxybenzo[*h*]quinoline catalysed by **1** in different solvents at 100 °C using 2 equivalents of $\text{PhI}(\text{OAc})_2$; Table S4-3. Transformation of benzo[*h*]quinoline to 10-alkoxybenzo[*h*]quinoline catalysed by **1** (1–3 mol%) in different solvents at 50 °C using 2 equivalents of $\text{PhI}(\text{OAc})_2$; Table S4-4. Transformation of benzo[*h*]quinoline to 10-alkoxybenzo[*h*]quinoline catalysed by $\text{PdI}_2(\text{dppf})$ **2** (1 or 2 mol%) in different solvents at 50 or 75 °C using 2 equivalents of $\text{PhI}(\text{OAc})_2$; Table S4-5. Transformation of 8-methylquinoline to 8-(methoxymethyl)quinoline using **1** or **2** as catalysts (1 or 2 mol% [Pd]) in different solvents at 50 °C using 2 equivalents of $\text{PhI}(\text{OAc})_2$; Table S5-1. Reaction conditions for the amination of *p*-bromobiphenyl with *p*-toluidine in CPME in the presence of $t\text{BuOK}$ at 100 °C used to generate data for DoE analysis; Table S5-2. Reaction profile for the amination of *p*-bromobiphenyl with *p*-toluidine against time. Conversion to the desired product was determined by ^1H NMR spectroscopy. References [22,24,28,29,42–49] are cited in the Supplementary Materials.

Author Contributions: K.A.J., G.E. and S.M. carried out experimental work and performed characterisation. A.J.P.W. performed the crystallography. K.A.J. and J.D.E.T.W.-E. wrote the initial draft of the manuscript with guidance and input from D.C.B. and A.S. All authors have read and agreed to the published version of the manuscript.

Funding: This research was funded by the Ministry of Higher Education, Malaysia and Universiti Teknologi MARA, Malaysia, grant number KPT(BS)820710105709, the Centre for Doctoral training in Next Generation Synthesis and Reaction Technology (Imperial College London, EP/S023232/1) and the Public Scholarship, Development, Disability and Maintenance Fund of the Republic of Slovenia (11010-136/215).

Data Availability Statement: The original contributions presented in the study are included in the article/supplementary material, further inquiries can be directed to the corresponding author.

Acknowledgments: K.A.J. would like to thank the Ministry of Higher Education, Malaysia and Universiti Teknologi MARA, Malaysia, for a scholarship on the Post Doctoral Training Scheme. S.M. gratefully acknowledges the provision of a studentship from the Centre for Doctoral training in Next Generation Synthesis and Reaction Technology. G.E. thanks the Public Scholarship, Development, Disability and Maintenance Fund of the Republic of Slovenia for a scholarship. K.A.J. would like to thank Max King for contributions to the research on the amination reactions.

Conflicts of Interest: The authors declare no conflicts of interest.

References

1. Johansson Seechurn, C.C.; Kitching, M.O.; Colacot, T.J.; Snieckus, V. Palladium-catalysed cross-coupling: A historical contextual perspective to the 2010 Nobel Prize. *Angew. Chem. Int. Ed.* **2012**, *51*, 5062–5085. [[CrossRef](#)] [[PubMed](#)]
2. Gensch, T.; Hopkinson, M.N.; Glorius, F.; Wencel-Delord, J. Mild metal-catalysed C–H activation: Examples and concepts. *Chem. Soc. Rev.* **2016**, *45*, 2900–2936. [[CrossRef](#)] [[PubMed](#)]
3. Lyons, T.W.; Sanford, M.S. Palladium-catalyzed ligand-directed C–H functionalisation reactions. *Chem. Rev.* **2010**, *110*, 1147–1169. [[CrossRef](#)] [[PubMed](#)]
4. Muci, A.R.; Buchwald, S.L. Practical Palladium Catalysts for C–N and C–O Bond Formation. In *Cross-Coupling Reactions; A Practical Guide* (2002); Miyaura, N., Ed.; Springer: Berlin/Heidelberg, Germany, 2002; Volume 219, pp. 131–209.
5. Gazvoda, M.; Dhanjee, H.H.; Rodriguez, J.; Brown, J.S.; Farquhar, C.E.; Truex, N.L.; Loas, A.; Buchwald, S.L.; Pentelute, B.L. Palladium-mediated incorporation of carboranes into small molecules, peptides, and proteins. *J. Am. Chem. Soc.* **2022**, *144*, 7852–7860. [[CrossRef](#)] [[PubMed](#)]
6. Reichert, E.C.; Feng, K.; Sather, A.C.; Buchwald, S.L. Pd-Catalyzed Amination of Base-Sensitive Five-Membered Heteroaryl Halides with Aliphatic Amines. *J. Am. Chem. Soc.* **2023**, *145*, 3323–3329. [[CrossRef](#)] [[PubMed](#)]

7. ACS Green Chemistry Institute: Endangered Elements. 2020. Available online: <https://www.acs.org/content/acs/en/greenchemistry/research-innovation/endangered-elements.html> (accessed on 22 April 2024).
8. Johnson Matthey. PGM Market Report. 2019, pp. 1–48. Available online: <http://www.platinum.matthey.com/services/market-research/pgm-market-reports> (accessed on 22 April 2024).
9. Nuss, P.; Eckelman, M.J. Life cycle assessment of metals: A scientific synthesis. *PLoS ONE* **2014**, *9*, e101298. [CrossRef] [PubMed]
10. Michałek, T.; Hessel, V.; Wojnicki, M. Production, recycling and economy of palladium: A critical review. *Materials* **2023**, *17*, 45. [CrossRef]
11. Macklin, M.G.; Thomas, C.J.; Mudbhakal, A.; Brewer, P.A.; Hudson-Edwards, K.A.; Lewin, J.; Scussolini, P.; Eilander, D.; Lechner, A.; Owen, J.; et al. Impacts of metal mining on river systems: A global assessment. *Science* **2023**, *381*, 1345–1350. [CrossRef]
12. Glaister, B.J.; Mudd, G.M. The environmental costs of platinum–PGM mining and sustainability: Is the glass half-full or half-empty? *Miner. Eng.* **2010**, *23*, 438–450. [CrossRef]
13. Yakoumis, I.; Panou, M.; Moschovi, A.M.; Panias, D. Recovery of platinum group metals from spent automotive catalysts: A review. *Cleaner Eng. Technol.* **2021**, *3*, 100112. [CrossRef]
14. Paiva, A.P.; Piedras, F.V.; Rodrigues, P.G.; Nogueira, C.A. Hydrometallurgical recovery of platinum-group metals from spent auto-catalysts—Focus on leaching and solvent extraction. *Sep. Purif. Technol.* **2022**, *286*, 120474. [CrossRef]
15. Wang, J.; Chen, H.; Hu, Z.; Yao, M.; Li, Y. A review on the Pd-based three-way catalyst. *Catal. Rev.* **2015**, *57*, 79–144. [CrossRef]
16. McCarthy, S.; Braddock, D.C.; Wilton-Ely, J.D.E.T. Strategies for sustainable palladium catalysis. *Coord. Chem. Rev.* **2021**, *442*, 213925. [CrossRef]
17. Hagelüken, B.C. Recycling the platinum group metals: A European perspective. *Platinum Met. Rev.* **2012**, *56*, 29–35. [CrossRef]
18. Dong, H.; Zhao, J.; Chen, J.; Wu, Y.; Li, B. Recovery of platinum group metals from spent catalysts: A review. *Int. J. Miner. Process.* **2015**, *145*, 108–113. [CrossRef]
19. Serpe, A.; Bigoli, F.; Cabras, M.C.; Fornasiero, P.; Graziani, M.; Mercuri, M.L.; Montini, T.; Pilia, L.; Trogu, E.F.; Deplano, P. Pd-dissolution through a mild and effective one-step reaction and its application for Pd-recovery from spent catalytic converters. *Chem. Commun.* **2005**, 1040–1042. [CrossRef] [PubMed]
20. Jantan, K.A.; Chan, K.W.; Melis, L.; White, A.J.P.; Marchiò, L.; Deplano, P.; Serpe, A.; Wilton-Ely, J.D.E.T. From recovered palladium to molecular and nanoscale catalysts. *ACS Sustain. Chem. Eng.* **2019**, *7*, 12389–12398. [CrossRef]
21. Jantan, K.A.; Kwok, C.Y.; Chan, K.W.; Marchiò, L.; White, A.J.P.; Deplano, P.; Serpe, A.; Wilton-Ely, J.D.E.T. From recovered metal waste to high-performance palladium catalysts. *Green Chem.* **2017**, *19*, 5846–5853. [CrossRef]
22. Dick, A.R.; Hull, K.L.; Sanford, M.S. A highly selective catalytic method for the oxidative functionalisation of C–H bonds. *J. Am. Chem. Soc.* **2004**, *126*, 2300–2301. [CrossRef]
23. McCarthy, S.; Desaunay, O.; Jie, A.L.; Hassatzky, M.; White, A.J.P.; Deplano, P.; Braddock, D.C.; Serpe, A.; Wilton-Ely, J.D.E.T. Homogeneous gold catalysis using complexes recovered from waste electronic equipment. *ACS Sustain. Chem. Eng.* **2022**, *10*, 15726–15734. [CrossRef]
24. Cuscusa, M.; Rigoldi, A.; Artizzu, F.; Cammi, R.; Fornasiero, P.; Deplano, P.; Marchiò, L.; Serpe, A. Ionic couple-driven palladium leaching by organic triiodide solutions. *ACS Sustain. Chem. Eng.* **2017**, *5*, 4359–4370. [CrossRef]
25. McCarthy, S.; Braddock, D.C.; Wilton-Ely, J.D.E.T. From waste to green applications: The use of recovered gold and palladium in catalysis. *Molecules* **2021**, *26*, 5217. [CrossRef] [PubMed]
26. Wilton-Ely, J.D.E.T. The use of recovered metal complexes in catalysis. *Johns. Matthey Technol. Rev.* **2023**, *67*, 300–302.
27. Wolfe, J.P.; Wagaw, S.; Buchwald, S.L. An improved catalyst system for aromatic carbon–nitrogen bond formation: The possible involvement of bis(phosphine) palladium complexes as key intermediates. *J. Am. Chem. Soc.* **1996**, *118*, 7215–7216. [CrossRef]
28. Driver, M.S.; Hartwig, J.F. A second-generation catalyst for aryl halide amination: Mixed secondary amines from aryl halides and primary amines catalysed by (DPPF)PdCl₂. *J. Am. Chem. Soc.* **1996**, *118*, 7217–7218. [CrossRef]
29. Colacot, T.J.; Qian, H.; Cea-Olivares, R.; Hernandez-Ortega, S. Synthesis, X-ray, spectroscopic and a preliminary Suzuki coupling screening studies of a complete series of dppfMX₂ (M = Pt, Pd; X = Cl, Br, I). *J. Organomet. Chem.* **2001**, *637*, 691–697. [CrossRef]
30. Topczewski, J.J.; Sanford, M.S. Carbon–hydrogen (C–H) bond activation at Pd IV: A Frontier in C–H functionalisation catalysis. *Chem. Sci.* **2015**, *6*, 70–76. [CrossRef] [PubMed]
31. Powers, D.C.; Ritter, T. Bimetallic Pd(III) complexes in palladium-catalysed carbon–heteroatom bond formation. *Nat. Chem.* **2009**, *1*, 302–309. [CrossRef] [PubMed]
32. Reetz, M.T.; Westermann, E. Phosphane-free palladium-catalysed coupling reactions: The decisive role of Pd nanoparticles. *Angew. Chem. Int. Ed.* **2000**, *39*, 165–168. [CrossRef]
33. Baumann, C.G.; De Ornellas, S.; Reeds, J.P.; Storr, T.E.; Williams, T.J.; Fairlamb, I.J.S. Formation and propagation of well-defined Pd nanoparticles (PdNPs) during C–H bond functionalisation of heteroarenes: Are nanoparticles a moribund form of Pd or an active catalytic species? *Tetrahedron* **2014**, *70*, 6174–6187. [CrossRef]
34. Reay, A.J.; Fairlamb, I.J.S. Catalytic C–H bond functionalisation chemistry: The case for quasi-heterogeneous catalysis. *Chem. Commun.* **2015**, *51*, 16289–16307. [CrossRef]
35. Guram, A.S.; Rennels, R.A.; Buchwald, S.L. A simple catalytic method for the conversion of aryl bromides to arylamines. *Angew. Chem. Int. Ed.* **1995**, *34*, 1348–1350. [CrossRef]
36. Wagaw, S.; Rennels, R.A.; Buchwald, S.L. Palladium-catalyzed coupling of optically active amines with aryl bromides. *J. Am. Chem. Soc.* **1997**, *119*, 8451–8458. [CrossRef]

37. Ali, M.H.; Buchwald, S.L. An improved method for the palladium-catalysed amination of aryl iodides. *J. Org. Chem.* **2001**, *66*, 2560–2565. [[CrossRef](#)] [[PubMed](#)]
38. Campeau, L.C.; Parisien, M.; Jean, A.; Fagnou, K. Catalytic direct arylation with aryl chlorides, bromides, and iodides: Intramolecular studies leading to new intermolecular reactions. *J. Am. Chem. Soc.* **2006**, *128*, 581–590. [[CrossRef](#)]
39. Forero-Cortés, P.A.; Haydl, A.M. The 25th anniversary of the Buchwald–Hartwig amination: Development, applications, and outlook. *Org. Process Res. Dev.* **2019**, *23*, 1478–1483. [[CrossRef](#)]
40. Azzena, U.; Carraro, M.; Pisano, L.; Monticelli, S.; Bartolotta, R.; Pace, V. Cyclopentyl methyl ether: An elective ecofriendly ethereal solvent in classical and modern organic chemistry. *ChemSusChem* **2019**, *12*, 40–70. [[CrossRef](#)] [[PubMed](#)]
41. Prat, D.; Wells, A.; Hayler, J.; Sneddon, H.; McElroy, C.R.; Abou-Shehada, S.; Dunn, P.J. CHEM21 selection guide of classical-and less classical-solvents. *Green Chem.* **2016**, *18*, 288–296. [[CrossRef](#)]
42. Dolomanov, O.V.; Bourhis, L.J.; Gildea, R.J.; Howard, J.A.K.; Puschmann, H. OLEX2: A Complete Structure Solution, Refinement and Analysis Program. *J. Appl. Cryst.* **2009**, *42*, 339–341. [[CrossRef](#)]
43. *SHELXTL v5.1*; Bruker AXS: Madison, WI, USA, 1998.
44. Sheldrick, G.M. Crystal structure refinement with SHELXL. *Acta Cryst.* **2015**, *C71*, 3–8.
45. Spek, A.L. (2003, 2009) PLATON, A Multipurpose Crystallographic Tool. *Acta Cryst.* **2015**, *C71*, 9–18.
46. Old, D.W.; Wolfe, J.P.; Buchwald, S.L. A Highly Active Catalyst for Palladium-Catalyzed Cross-Coupling Reactions: Room-Temperature Suzuki Couplings and Amination of Unactivated Aryl Chlorides. *J. Am. Chem. Soc.* **1998**, *120*, 9722–9723. [[CrossRef](#)]
47. Wolfe, J.P.; Tomori, H.; Sadighi, J.P.; Yin, J.; Buchwald, S.J. Simple, Efficient Catalyst System for the Palladium-Catalyzed Amination of Aryl Chlorides, Bromides, and Triflates. *J. Org. Chem.* **2000**, *65*, 1158–1174. [[CrossRef](#)]
48. Semeniuchenko, V.; Braje, W.M.; Organ, M.G. Sodium Butylated Hydroxytoluene: A Functional Group Tolerant, Eco-Friendly Base for Solvent-Free, Pd-Catalysed Amination. *Chem. Eur. J.* **2021**, *27*, 12535–12539. [[CrossRef](#)] [[PubMed](#)]
49. Hajra, A.; Wei, Y.; Yoshikai, N. Palladium-Catalyzed Aerobic Dehydrogenative Aromatization of Cyclohexanone Imines to Arylamines. *Org. Lett.* **2012**, *14*, 5488–5491. [[CrossRef](#)] [[PubMed](#)]

Disclaimer/Publisher’s Note: The statements, opinions and data contained in all publications are solely those of the individual author(s) and contributor(s) and not of MDPI and/or the editor(s). MDPI and/or the editor(s) disclaim responsibility for any injury to people or property resulting from any ideas, methods, instructions or products referred to in the content.